THESIS FOR THE DEGREE OF LICENTIATE OF ENGINEERING

Sustained and triggered release by microencapsulation

VIKTOR ERIKSSON

Department of Chemistry and Chemical Engineering
Chalmers University of Technology
Gothenburg, Sweden, 2021

Sustained and triggered release by microencapsulation

VIKTOR ERIKSSON

Licentiatuppsatser vid Institutionen för kemi och kemiteknik
Chalmers tekniska högskola
Nr 2021:15

Department of Chemistry and Chemical Engineering
Chalmers University of Technology
SE-412 96 Gothenburg, Sweden
Phone: +46 (0)31 772 1000
www.chalmers.se

Cover: illustration of two microcapsules showing sustained release (green) and triggered release (blue), respectively.

Printed by Chalmers Digitaltryck
Gothenburg, Sweden, September 2021

Sustained and triggered release by microencapsulation
Viktor Eriksson
Department of Chemistry and Chemical Engineering
Chalmers University of Technology

Abstract

Uncontrolled growth of microorganisms is problematic in areas ranging from wound care to aquaculture and ship hulls. In chronic and hard-to-heal wounds, a bacterial biofilm can impair wound healing. The growth of marine microorganisms, so-called biofouling, on equipment used in aquaculture can decrease productivity and thereby result in a loss of revenue. To counteract these problems and minimize microbial growth, antimicrobial substances have been developed. For efficient use of these antimicrobial substances that enables long-term protection without excessive use, their release from materials should be controlled.

In this work, microencapsulation was used as a means of controlling the rate at which a model hydrophobic substance was released in two different ways. A slow *sustained release* microparticle system with a complete release over a period of weeks was developed. These microcapsules were also incorporated into cellulose fibers, to produce a nonwoven material possessing controlled release properties. As a complement to this, a fast *triggered release* system was developed where a significant release could be seen within minutes of the trigger event.

Through a combination of these two types of controlled release, a hypothetical release profile could be tailored to fit specific applications. The triggered release microparticles could initially increase the antimicrobial concentration above a certain effective concentration, and the sustained release microparticles would maintain the concentration above the effective concentration for a prolonged time. The use in a nonwoven fiber material was illustrated in this work, although use in e.g. continuous fibers or painted coatings could also easily be conceived.

Keywords: Microencapsulation, controlled release, cellulose, solution blown.

List of Publications

I Solution-spinning of a collection of micro- and nanocarrier-functionalized polysaccharide fibers
Hanna Ulmefors, Ting Yang Nilsson, Viktor Eriksson, Gustav Eriksson, Lars Evenäs, and Markus Andersson Trojer
Manuscript

II Microencapsulation for controlled release of model active substances from cellulose nonwovens
Viktor Eriksson, Jules Mistral, Ting Yang Nilsson, Markus Andersson Trojer, and Lars Evenäs
Manuscript

III Formulation of polyphthalaldehyde microcapsules for immediate UV-light triggered release
Viktor Eriksson, Markus Andersson Trojer, Szilvia Vavra, Mats Hulander, and Lars Nordstierna
Journal of Colloid and Interface Science 579 (2020): 645-653

My Contributions to the Publications

Paper I
Co-author. Parts of sample preparation for the cellulose-based fibers. Optical and fluorescence microscopy analysis of most materials.

Paper II
Main author. All experimental work, except SEM and confocal microscopy.

Paper III
Main author. All experimental work, except SEM and degradation studies using IR-spectroscopy.

List of Figures

Contents

1

Introduction

There is a fight against the uncontrolled growth of microorganisms on surfaces in several sectors. In non-healing chronic wounds, bacterial colonization can lead to biofilm formation which in turn can impair wound healing and even lead to an increased mortality rate from sepsis. Such biofilm formation has been seen in a large fraction of studied chronic wounds [1]. In both aquaculture and on ship hulls, a similar problem of undesired microbial growth, biofouling, can be observed [2, 3]. Biofouling by aquatic microorganisms on these surfaces can lead to sub-optimal performance and loss of revenue. In aquaculture, the consequences of biofouling are estimated to make up at least 5-10% of the total production cost.

To combat this uncontrolled growth of microorganisms, a large effort has been put into developing chemicals capable of killing the microorganisms in order to prevent their growth [4, 5]. Today, small organic molecules such as quaternary ammonium compounds and isothiazolinones are commonly used for this purpose in a wide range of consumer products [6, 7]. Only developing new antimicrobial substances is however not enough. There is also a need for optimizing how they are loaded into and released from materials. A common problem with many of the products containing these substances, such as wound dressings and painted surfaces, is the lack of long-term efficacy. Due to the small molecular size of the antimicrobials, their diffusivity is large. Thereby, they are readily transported out of the materials where their antimicrobial effect is desired, and then easily washed away from the surfaces. To counteract this, an excess of the antimicrobial substance is commonly

added. While extending the time frame for release slightly, it also leads to an excessive initial release rate. Any antimicrobial substance released after reaching below a certain effective surface concentration is simply wasted.

The widespread and extensive use of these antimicrobial substances has led to an increasing prevalence of resistance in bacteria [8]. To keep this from further increasing, the exposure to the antimicrobials should be minimized. There is also an economic incentive behind decreasing the amount of expensive antimicrobial substances loaded into materials. Decreasing the used amount of antimicrobial substance has to be done without decreasing the efficacy. By having strategies for controlling the release of antimicrobials, this could be achieved. The initially high and excessive dosage could be avoided while still providing sufficient efficacy over time. One strategy for achieving such controlled release is microencapsulation. By loading the antimicrobials into micro-sized particles, their release rate could be precisely tuned. The microparticles could then in turn be embedded in the materials of interest, thereby giving the materials a controlled release functionality.

1.1 Purpose and Objectives

To reach the desired release rate of actives, precisely tuning the release is needed. Initially, a sufficiently large dose may need to be rapidly released in order to reach effective concentrations. At the same time, a slow and extended release is desired to maintain efficacy over time. To reach the desired release rate of actives, multiple controlled release systems may therefore be necessary. A *sustained release* that is slow and continuous is required for long-term efficacy. At the same time, an initial *triggered release* may be required to initially release a sufficient amount to reach an effective concentration.

The objectives of this work were therefore divided into two parts: (*i*) developing strategies for different release rates from microparticles and (*ii*) creating a macroscopic material possessing these controlled release properties.

To cover these two types of release characteristics, the encapsulation and sustained release of a model substance was investigated in Paper I and II. The hydrophobic model substance pyrene was encapsulated in these materials. Microspheres for

sustained release of the model substance were formulated and immobilized in cellulose fibers, resulting in a nonwoven material possessing sustained release properties. In Paper III, a microcapsule system for immediate triggered release of the same model substance was investigated. The UV light and acid-triggered release was evaluated both from microcapsules in water suspension and from microcapsules dried onto a glass substrate.

2

Controlled Release of Active Substances

Microcapsules are micrometer-sized particles where an active substance is packaged within a shell material for subsequent controlled release [9]. In the 1960s, so-called microcapsules began appearing in carbonless copy paper [10]. Here, dye-loaded microcapsules embedded in the copy paper enabled a triggered release of the encapsulated dye when the paper was being used. Since the 1960s, a multitude of release systems has also been developed for the controlled delivery of pharmaceuticals. Macroscopic devices were initially developed [11], but microcapsules rapidly increased in popularity. The highly adaptable microcapsule systems allow for a wide variety of different release profiles to be achieved. These range from fast release triggered by various external stimuli, such as a change in pH-value or light irradiation, [12] to slow and sustained release [13].

In this work, two main classes of microparticles are considered: microspheres and microcapsules [13]. A microsphere is the simplest morphology in which the active substance is distributed homogeneously throughout a spherical polymer matrix. A more intricate morphology is that of a core-shell microcapsule. Here, a solid polymer phase encapsulates a core oil into which an active substance is dissolved. These two morphologies are illustrated in Figure 2.1a) and b), respectively. Several routes can be followed to prepare such microparticles, including interfacial polymerization and internal phase separation among others [14]. In this work, only microparticles prepared by internal phase separation are discussed. In short, this method is based on creating an oil-in-water emulsion. In the oil phase, the microcapsule shell and

core materials are dissolved in a volatile solvent with low water solubility. When evaporating the volatile solvent, an internal phase separation takes place inside the emulsion droplets which creates the microcapsules [15].

2.1 Morphologies of Microcapsules

There is a multitude of conceivable two-phase microcapsule morphologies, some of which are presented in Figure 2.1. The morphology of a microcapsule system prepared by internal phase separation can be predicted mathematically by using spreading coefficients for the different phases. These spreading coefficients are in turn dependent on the interfacial tensions between the relevant microcapsule phases. Torza and Mason [16] developed this concept for determining the morphologies in a system of three immiscible liquids. Both Sundberg et al. [17] as well as Loxley and Vincent [15] finally expanded this concept further to also predict the morphologies in three-phase systems containing a solid polymer as in the case of a microcapsule. The spreading coefficient S_i for phase i in a system of three immiscible phases i, j, and k can be calculated from the three different interfacial tensions between the phases,

$$S_i = \gamma_{jk} - (\gamma_{ij} + \gamma_{ik}). \tag{2.1}$$

For a typical microcapsule system, spreading coefficients for the following three phases must be considered: the oil phase (S_o), the water phase (S_w), and the polymer phase (S_p). Four different combinations of these spreading coefficients are possible, as shown by Equations 2.2 - 2.5.

$$S_\mathrm{o} < 0; \quad S_\mathrm{w} < 0; \quad S_\mathrm{p} > 0, \tag{2.2}$$
$$S_\mathrm{o} < 0; \quad S_\mathrm{w} > 0; \quad S_\mathrm{p} < 0, \tag{2.3}$$
$$S_\mathrm{o} > 0; \quad S_\mathrm{w} < 0; \quad S_\mathrm{p} < 0, \tag{2.4}$$
$$S_\mathrm{o} < 0; \quad S_\mathrm{w} < 0; \quad S_\mathrm{p} < 0. \tag{2.5}$$

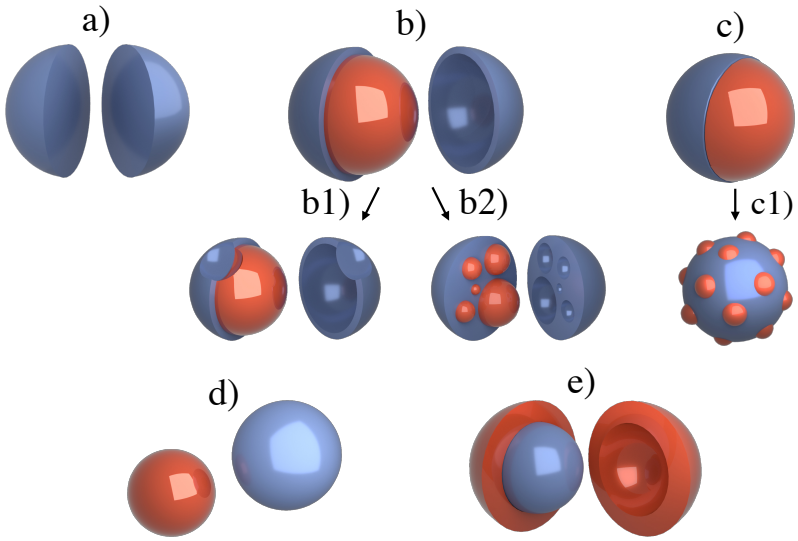

Figure 2.1: Illustration of a a) microsphere, along with conceivable two-phase microcapsule morphologies: b) core-shell, b1) *blueberry*, b2) multi-core, c) *acorn*, c1) *raspberry*, d) droplet separation, e) inverted core-shell. The polymer phase is shown in blue and the oil phase in red.

Each of these sets of spreading coefficients corresponds to a different thermodynamically predicted microcapsule morphology. The core-shell particle in Figure 2.1b) can be predicted by the set of spreading coefficients in Equation 2.2. This is also the only morphology in which the oil is successfully encapsulated within the microcapsule. The acorn morphology in Figure 2.1c) is mathematically predicted by Equation 2.5. In Figure 2.1d) a complete droplet separation is shown, predicted by Equation 2.3. Finally, an inverted core-shell particle (Figure 2.1e)) where the oil phase surrounds the polymer shell is predicted thermodynamically by Equation 2.4. It can thus be seen that in order to successfully encapsulate the oil phase inside a core-shell particle, the core oil phase must be sufficiently hydrophobic as compared to the desired polymer shell.

Apart from these four main types of microparticles, several other morphologies are found in the literature that cannot be directly described by the classical thermodynamic spreading coefficients. Both the dimpled core-shell particle,

so-called *blueberry* microcapsule, as shown in Figure 2.1b1) [18, 19] and the multi-core particle in Figure 2.1b2) [20] have been reported and should both fulfill the thermodynamic conditions for a core-shell particle while still deviating significantly in their morphology. Similarly, the *raspberry*-like microparticle [21] in Figure 2.1d1) should fulfill the spreading conditions for an acorn microparticle.

2.2 Sustained Release

For pharmaceuticals intended to be administered slowly and continuously [22] or for long-term biofouling protection of coatings [23], a sustained release profile of actives is of great importance. Through microencapsulation, the microparticles are supposed to act as the rate-limiting barrier controlling the release rate of actives. There are several mechanisms by which the actives can be released from the microparticles. When biodegradable microcapsule materials are used, such as polylactide-based polyesters, both diffusion through the polymer matrix and degradation of the matrix itself can affect the release rate [24]. For small molecules, such as biocides for antifouling, the release is usually governed by diffusion through the polymer matrix [25]. The diffusion of larger molecules, such as peptides and proteins, through a polymer matrix is usually negligible on the time scales relevant for controlled release. Hence, their release is often to a larger extent dependent on the degradation of the polymer matrix. During degradation the polymer starts disintegrating, forming water-filled pores inside the matrix through which the actives can diffuse out [24].

2.3 Triggered Release

From a sustained release system, the active is being released slowly and continuously. By examining the release profile from such a system, it can be seen that a certain amount of time is needed to reach an effective concentration of the active substance. A system where an antibacterial substance is released from a wound dressing in a chronic wound can be considered as an example. For a system relying solely on sustained release, the initial concentration of the antibacterial agent in the wound would be far below the effective concentration where the growth

of bacteria is prevented. Here, a system comprising both triggered and sustained release could be utilized. By triggering the release of a fraction of the antibacterial substance, the concentration in the wound could be brought above the effective concentration. The other fraction of antibacterial substance being released slowly via sustained release would then maintain the concentration above the effective concentration for an extended time.

Several approaches for triggered release of actives have been presented, relying on a multitude of different triggers. These include changes in pH, ultraviolet, and near-infrared light among others [26–29]. This functionality can be used to e.g. deliver pharmaceuticals in specific regions of the gastrointestinal tract on the basis of different pH-values [30]. The release of cosmetics and herbicides for agriculture could be triggered by UV light exposure due to the natural UV light abundance in those application areas [12]. The light-triggered release also has the advantage of being possible to control remotely, without relying on physical changes such as a difference in pH value or temperature.

One polymer with interesting properties for triggered release is polyphthalaldehyde (PPA). Its synthesis was first described in the 1960s [31] and has since then been investigated for its possibility to be used as a resist in photolithography [32]. Due to its low ceiling temperature of -43 °C, it rapidly depolymerizes. Through various end-caps, the polymer can be stabilized and the depolymerization hindered. However, once the depolymerization is triggered it rapidly reverts into its monomeric constituents [33]. PPA microcapsules sensitive to acid have been formulated previously [34], and fluoride-sensitive microcapsules have been formulated by selecting a fluoride-sensitive end-cap for the PPA [35]. There is also an inherent UV light triggered degradation of PPA [36].

2.4 Macroscopic Controlled Release Materials

Microencapsulation is a promising route for the delivery of drugs, either for parenteral or oral formulations [37–39]. In for example a wound dressing, however, the microcapsules would easily be washed away from the area where they would be applied, eliminating the effect from active substances. To counteract this, a macroscopic material from which controlled release can be achieved is required.

Both fiber materials and hydrogels have previously been used for these purposes [40–43]. Many of these materials do however not provide a sufficient degree of control of the release rate of actives, as pointed out previously. By immobilizing microcapsules in a fiber material, the advantages of both materials could be combined. Microcapsules would control the release rate of actives, whereas the fiber material would provide the desired structural integrity.

Several fossil-based raw materials are available for producing fiber materials with the desired properties. There are, however, several bio-based and renewable polysaccharides available as replacements for these. Cellulose is the most abundant biopolymer on Earth, and is hence an attractive alternative for producing the previously mentioned fiber materials [44]. Chitosan and alginate are other underused raw materials of interest for these applications [45, 46].

3

Experimental

3.1 Microcapsule Formulation

The formulation procedure for preparing two-phase oil core-polymer shell microcapsules in Paper III was based on internal phase separation by solvent evaporation, described by Vincent and Loxley [15]. The core oil hexadecane, shell polymer polyphthalaldehyde (PPA), and the active substance pyrene were dissolved in the volatile solvent dichloromethane (DCM). Following this, an oil-in-water emulsion was prepared by dispersing the DCM solution in a water solution containing a polymeric dispersant under high-speed shearing. After preparing this emulsion, it was transferred to a vial and left under gentle magnetic stirring for at least 10 hours for the DCM to evaporate. During this evaporation, the immiscible core and shell materials phase-separated within the emulsion droplets as the fraction of volatile solvent decreased, leading to the desired core-shell morphology. This is illustrated schematically in Figure 3.1. In Paper I and II, PPA was replaced with the biodegradable polyester poly(D,L-lactide-*co*-glycolide) (PLGA). The solid microspheres used were formulated following a similar procedure, but with the modification of omitting the core oil and replacing it with an equal amount of shell polymer.

Several conditions need to be fulfilled to prepare microcapsules by the internal phase separation method. Starting with the volatile solvent, two conditions should be fulfilled. First of all, it must dissolve all of the mentioned microparticle

components. Secondly, it should have a slight water solubility to facilitate its evaporation. During evaporation from the prepared emulsion, the volatile solvent should be transported from the emulsion droplets to the surrounding continuous water phase towards the water surface where it can evaporate. By having a slight water solubility of the volatile solvent, the evaporation rate can be increased. Two solvents possessing these properties are DCM and chloroform.

Looking at the microcapsule materials, several conditions need to be fulfilled as well. Naturally, the core and shell material must be immiscible in each other to produce a two-phase microcapsule. The oil core must also be sufficiently hydrophobic as compared to the shell material in order to produce the desired core-shell morphology, as described by the spreading conditions in Equation 2.2 - 2.5.

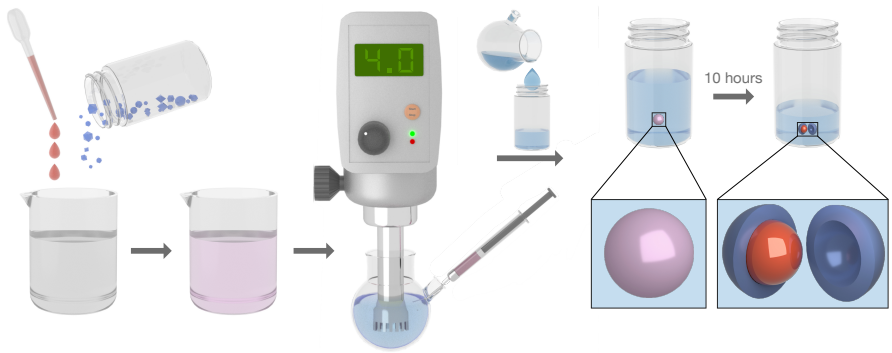

Figure 3.1: Schematic illustration of the formulation procedure for producing microparticles.

3.2 Interfacial Tensions and the van Oss Formalism

As described in Equation 2.2 - 2.5, the morphology of a two-phase microcapsule can be predicted by spreading coefficients based on the interfacial tensions between the two phases in the microcapsule and the outer water phase, respectively. To predict the morphologies of the formulated microcapsules in Paper III, the relevant interfacial tensions were measured for these microcapsule systems. The interfacial tension between two liquid phases was measured directly by the pendant drop technique. The curvature of a droplet hanging from a needle is dependent on the interfacial tension between the droplet and the surrounding medium, among other

factors. The interfacial tension for such a pendant drop can be expressed as

$$\gamma = \frac{\Delta\rho g R_0}{\beta} \tag{3.1}$$

where $\Delta\rho$ is the density difference between the droplet and its surrounding medium, g is the gravitational constant, R_0 is the curvature radius at the droplet apex and β is a shape factor.

The interfacial tension between the solid polymer and the liquid oil and water phase respectively cannot be measured directly. Instead, an indirect method was required. The methodology developed by van Oss and coworkers [47] was used in Paper III for determining the surface energy of the solid polymer phase. The methodology is based on measuring the contact angles of several well-known test liquids on the substrate of interest. Any interfacial tension can be divided into Lifshitz-van der Waals (LW) interactions and acid-base (AB) interactions, Equation 3.2. The acid-base interactions can be further divided into electron acceptor (γ_i^+) and electron donor (γ_i^-) interactions according to Equation 3.3. The contact angle θ was measured on the polymer substrate for each of the test liquids. By nonlinear regression the polymer surface energy γ_S^{tot} could be determined through Equations 3.2 - 3.4. By then measuring contact angles for the oil and water phases of interest on the polymer surface, their interfacial tensions could be determined through Equation 3.5, knowing both the surface tension of the liquid of interest (γ_L^{tot}) and the surface energy of the polymer substrate.

$$\gamma_i^{tot} = \gamma_i^{LW} + \gamma_i^{AB} \tag{3.2}$$

$$\gamma_i^{AB} = 2\sqrt{\gamma_i^+ \gamma_i^-} \tag{3.3}$$

$$1 + \cos(\theta)\gamma_L^{tot} = 2\left[\left(\gamma_S^{LW}\gamma_L^{LW}\right)^{1/2} + \left(\gamma_S^+\gamma_L^-\right)^{1/2} + \left(\gamma_S^-\gamma_L^+\right)^{1/2}\right] \tag{3.4}$$

$$\gamma_S^{tot} = \gamma_{SL} + \gamma_L^{tot}\cos(\theta) \tag{3.5}$$

3.3 Solution Blowing

To produce the cellulose nonwoven materials used in Paper I and II, solution blowing was used [48]. Microcrystalline cellulose, used for its lower average molecular weight than regular dissolving pulp, was dried at 80 °C for one hour. The cellulose was then mixed with 1-ethyl-3-methylimidazolium acetate (EMIMAc) under overhead stirring in a glass reactor at room temperature. Pyrene was also added to the EMIMAc when preparing the fiber samples containing freely dispersed pyrene. Once all large clusters of cellulose particles were well-dispersed in the liquid, the mixture was heated to 70 °C for one hour in order to dissolve the cellulose. After complete dissolution, the prepared dope solution was cooled down to room temperature. Similar dope solutions were used for the wet spun fibers.

For the fiber samples containing microparticles, the particles were added to the dope solution after allowing it to cool down to room temperature. The dope solution is water sensitive, and a too large amount of water in it will coagulate the dissolved cellulose. Since the microparticles were prepared in a water suspension at 2 wt.%, it was therefore important to minimize the water content in the microparticle suspension. By careful centrifugation, the microparticles were sedimented to yield a microparticle concentration of approximately 50 wt.%. This sediment was then redispersed in a small amount of EMIMAc before being added to the dope solution. It was important that the dope solution had cooled down to room temperature before adding the microparticles. The glass transition temperature of the hydrated PLGA microparticles is around 30 °C [49] meaning that the microparticles may have deformed significantly during shearing at elevated temperatures.

After preparing the dope solution, solution blowing was used to produce the different nonwoven materials used for subsequent release measurements. The dope solution was added to a cylinder and pushed through 220 µm capillaries by a piston. After being extruded through the capillaries, compressed air stretched the fibers further in the air gap between the spinneret and coagulation bath. Once the fibers reached the coagulation bath, they rapidly coagulated and were collected onto a rotating metal drum. The experimental setup used for solution blowing is illustrated in Figure 3.2.

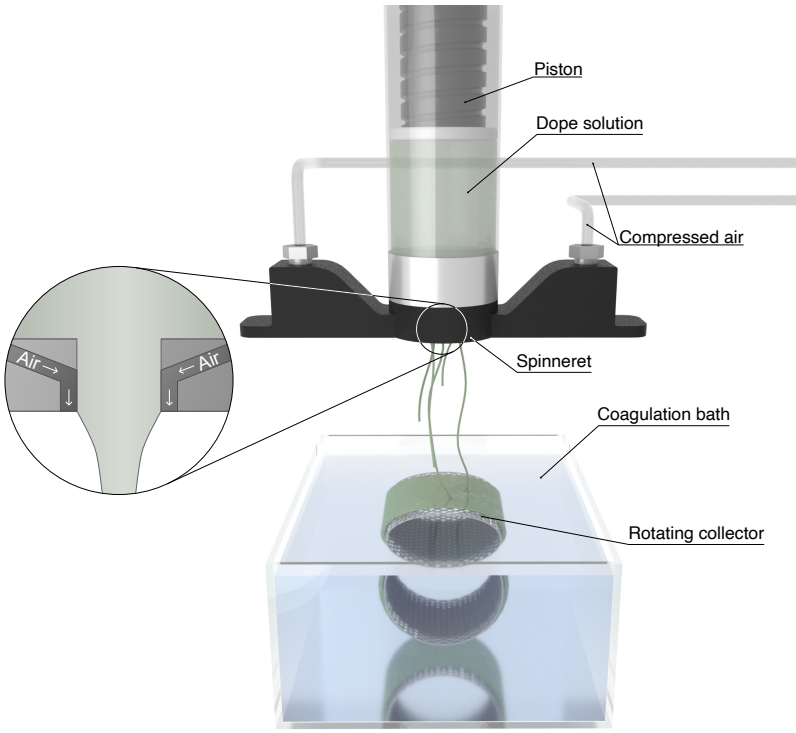

Figure 3.2: Illustration of the experimental setup used for preparing nonwovens by solution blowing.

Normally, dissolving pulp is used for preparing the dope solutions used for solution blowing. This results in a dope solution with significantly higher viscosity as compared to dope solutions prepared with microcrystalline cellulose. The solution blowing is then usually done while keeping the dope solution heated at up to 70 °C [48], which decreases its viscosity. As mentioned previously, the microparticles are temperature sensitive as a result of their low glass transition temperature. Hence, elevated temperatures could not be used during solution blowing. Cosolvents such as dimethylsulfoxide or methylimidazole could be added to decrease the dope viscosity and prevent die swelling [50]. Many of these EMIMAc/cosolvent mixtures do however disintegrate the PLGA microparticles entirely. Based on these considerations, a dope solution prepared with the lower

molecular weight microcrystalline cellulose was used for microparticle-loaded fibers.

3.4 Microscopy Characterization

To understand the structure of prepared microparticles, as well as the nonwoven fiber materials, several microscopy techniques were employed. Knowing the size and morphologies of the prepared materials is of paramount importance for subsequent analyses.

Optical brightfield microscopy was used to determine size distributions of both microspheres (Paper II and III) and fibers (Paper II). Pyrene, used as a model active substance, shows a strong blue fluorescence which allows for further characterization using fluorescence microscopy. The fiber surface and distribution of microspheres within the fiber material were further visualized by confocal and scanning electron microscopy.

To elucidate microcapsule morphologies in Paper III, fluorescence microscopy was also used. The polymer PPA used as a shell material exhibited green autofluorescence. In the core oil, pyrene was dissolved which displays a blue fluorescence. By overlaying an optical micrograph with blue and green fluorescence micrographs, composite images could be obtained from which the microcapsule morphologies could be elucidated. In post-processing, the green tone was shifted to red for a more clear differentiation between the two fluorescent phases.

3.5 Release Measurements

The sustained release of pyrene from nonwoven fiber materials and microspheres in Paper II was evaluated in a water solution. So-called sink conditions were desired during these tests, meaning that the concentration of pyrene had to be sufficiently far below the saturation concentration in the liquid. Due to the hydrophobic nature of pyrene, its water solubility is very low. The nonionic surfactant Brij L23 was therefore added to the release medium, solubilizing pyrene and resulting in desired sink conditions. Without this, the partition coefficient for pyrene between a

microsphere and its surrounding aqueous phase would significantly affect the release rate [51, 52].

During the release experiments, a piece of the nonwoven fiber material or a small amount of the microsphere suspension was added to a large, stirred volume of the release medium. Aliquots of the release medium were taken out at given times and filtered through syringe filters to remove microspheres or fiber debris, stopping the continuous release of pyrene. By UV-visible spectroscopy, the amount of released pyrene at each time point could be determined using the Beer-Lambert law, $A = \varepsilon cl$. Here A is the measured absorbance, ε is the molar absorptivity, c is the concentration and l is the path-length of the cuvette.

To determine the total loading of pyrene for both the microspheres in water suspension and the fiber materials, a similar approach was used. After completing the release experiment, ethanol was added to the samples. This is a much better solvent for pyrene, and it swells both the fibers and microspheres, allowing for fast and complete extraction of any remaining pyrene. The samples were left overnight to ensure that all pyrene was extracted, then they were filtered and analyzed by UV-vis spectroscopy.

The triggered release in Paper III was instead evaluated qualitatively. The microspheres were irradiated by UV light from the fluorescence microscope. This way, the release of the interior core oil could be monitored *in situ*. The triggered release was performed both on microcapsules in water suspension and on dry microcapsules placed on a glass slide.

3.6 Modelling Sustained Release

The diffusion of a small molecule inside a matrix can be modelled by the diffusion equation. In its simplest form, the equation can be reduced to a one-dimensional problem. For such a one-dimensional problem, the diffusion equation is expressed as

$$\frac{\partial C}{\partial t} = D\frac{\partial^2 C}{\partial x^2} \tag{3.6}$$

where C is the concentration of diffusing substance, t is time, D is the diffusion coefficient inside the studied geometry and x is a characteristic length. It is convenient to express the release in terms of fractional release, $m(t)/m_{\text{tot}}$, rather than as a concentration.

3.6.1 Microspheres

The diffusion equation (Equation 3.6) is described on a spherical geometry by Crank [52]. This gives the possibility of modelling the fractional release (f_{s}) of an active substance from microspheres,

$$f_{\text{s}}(r,t) = \frac{\alpha_{\text{s}}}{1+\alpha_{\text{s}}}\left[1 - \sum_{n=1}^{\infty} \frac{6\alpha_{\text{s}}(\alpha_{\text{s}}+1)}{9+9\alpha_{\text{s}}+q_{\text{s},n}^2\alpha_{\text{s}}^2} \exp\left(-\frac{Dq_{\text{s},n}^2 t}{r^2}\right)\right]. \tag{3.7}$$

Here, r is the radius of the sphere and α_{s} is expressed as

$$\alpha_{\text{s}} = \frac{V_{\text{sink}}}{V_{\text{sphere}}K} \tag{3.8}$$

with K as the partition coefficient of the diffusing substance between the sphere and the surrounding release medium. V_{sink} and V_{sphere} are the volumes of release medium and microspheres, respectively. $q_{\text{s},n}$ is defined as the n:th non-zero positive root of

$$\tan q_{\text{s},n} = \frac{3q_{\text{s},n}}{3+\alpha_{\text{s}}q_{\text{s},n}^2}. \tag{3.9}$$

Microspheres used for controlled release are never monodisperse, but always have a polydispersity. Therefore, a single radius r cannot be used in equation 3.7. Instead the final expression for the fractional release must be weighted according to the polydispersity,

$$\frac{m(t)}{m_{\text{tot}}} = \frac{\int f_{\text{s}}(r,t)p(r)r^3\,dr}{\int p(r)r^3\,dr}. \tag{3.10}$$

The probability density function $p(r)$ used in Equation 3.10 normally follows a log-normal distribution function [53],

$$p(r) = \frac{1}{r\sigma\sqrt{2\pi}} \exp\left(-\frac{(\ln x - \mu)^2}{2\sigma^2}\right), \tag{3.11}$$

where μ and σ are the mean and standard deviation of the logarithmized radius.

3.6.2 Fiber Materials

Similar to release from microspheres, the diffusion from fibers can also be mathematically modelled. The fractional release from a fiber (f_{c}) in which the diffusing substance is homogeneously distributed can be modelled with a cylindrical geometry. This is described by Crank [52],

$$f_{\text{c}}(r,t) = \frac{\alpha_{\text{c}}}{1+\alpha_{\text{c}}}\left[1 - \sum_{n=1}^{\infty} \frac{4\alpha_{\text{c}}(\alpha_{\text{c}}+1)}{4+4\alpha_{\text{c}}+q_{\text{c},n}^2\alpha_{\text{c}}^2} \exp\left(-\frac{Dq_{\text{c},n}^2 t}{a^2}\right)\right], \tag{3.12}$$

where a is the radius of the fiber. The parameter α_{c} is defined as

$$\alpha_{\text{c}} = \frac{V_{\text{sink}}}{V_{\text{cyl}}K} \tag{3.13}$$

with V_{cyl} being the volume of the cylinder. For a cylinder, $q_{\text{c},n}$ is defined as the n:th non-zero positive root of

$$\alpha_c q_{c,n} J_0(q_{c,n}) + 2J_1(q_{c,n}) = 0. \tag{3.14}$$

Here, J_0 and J_1 are the Bessel functions of the first kind of order 0 and 1, respectively. Similar to the microspheres, polydispersity in the fiber radii has to be taken into account:

$$\frac{m(t)}{m_{\text{tot}}} = \frac{\int f_c(a,t)p(a)a^2\,da}{\int p(a)a^2\,da}. \tag{3.15}$$

When the active substance is adsorbed onto the fibers, two different components are required to mathematically describe the release. The active substance on the surface of the fiber will be rapidly released, here denoted as a burst release that is assumed to be a zero-order release. Parts of the active substance will permeate into the fiber during impregnation, from which it will be slowly released through diffusion. The fractional release can therefore be expressed as

$$f(n) = \begin{cases} p_b k_b t + (1-p_b) f_p(L,t), & \text{if } t < t_b \\ p_b k_b t_b + (1-p_b) f_p(L,t), & \text{if } t \geq t_b \end{cases} \tag{3.16}$$

with p_b defined as the burst fraction, k_b as the rate constant for the burst release, and t_b as the time during which the burst release occurs. The slower, diffusional contribution to the release $f_p(L,t)$ can be approximated as diffusion from a plane sheet [52],

$$f_p(L,t) = 1 - \sum_{n=0}^{\infty} \frac{8}{(2n+1)^2\pi^2} \exp\left(-\frac{D(2n+1)^2\pi^2 t}{4L^2}\right), \tag{3.17}$$

where L is the thickness of the sheet.

4

Results and Discussion

4.1 Sustained Release Systems

In Paper I, a multitude of microparticle-functionalized fiber materials were prepared. These can be divided into two fundamentally different types of fiber materials: nonwovens and continuous fiber filaments. The pyrene release rate from the nonwoven fiber materials was later evaluated in an aqueous solution in Paper II.

4.1.1 Fiber Preparation

Solution blowing and wet spinning was used to prepare the two different types of fiber materials. Through solution blowing, a nonwoven, i.e. a disordered network of cellulose fibers, was created. Wet spinning, on the other hand, created long and continuous fiber filaments. These two fiber material types are shown in Figure 4.1. Both core-shell particles, as well as the more simple microspheres, with diameters around 10 μm were successfully immobilized within these fibers. Wet spun cellulose fibers loaded with PLGA core-shell particles are shown in Figure 4.2. The microcapsules were intact and retained their core-shell structure after the fiber spinning, as seen in Figure 4.2a). A slight deformation of the microcapsules could be seen after wet spinning, possibly as a result of the shear forces involved during the extrusion of the dope solution through the spinneret. From the fluorescence

micrographs in Figure 4.2b), further evidence that the microcapsules remained intact was seen. The strong fluorescence in the microcapsule cores indicated that the microcapsule shells had not broken and that the cores, and the pyrene dissolved in them, were still successfully encapsulated within the capsules.

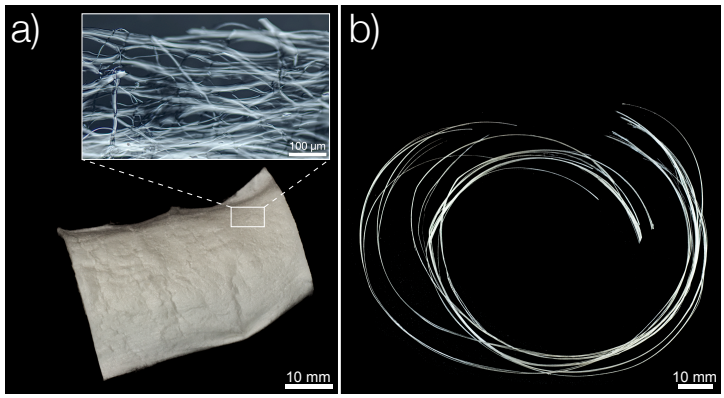

Figure 4.1: Photographs of fiber materials prepared by a) solution blowing and b) wet spinning. The inset in a) shows a magnified differential interference contrast micrograph of the nonwoven.

Solution blown cellulose fibers containing pyrene-loaded microspheres were also prepared in Paper I, and further investigated in Paper II as a sustained release system. The sustained release of pyrene was not only evaluated from nonwovens containing pyrene-loaded microspheres. For comparison, pyrene was also loaded by a more simple impregnation in two different ways: by surface impregnation and by freely dispersing pyrene throughout the entire fiber cross-section. The three materials are shown in Figure 4.3, visualized by both optical and fluorescence microscopy.

Comparing the materials where pyrene is loaded within the fibers, i.e. the microencapsulated and freely dispersed pyrene, a much higher loading efficiency was seen during microencapsulation. In Paper I it was shown that only 7% of the freely dispersed pyrene remain in the fiber, whereas 95% was remaining in the fiber by microencapsulation. Pyrene is highly hydrophobic with a water solubility of only 0.1 mg/L [54]. A plausible explanation for the large loss of pyrene is the mass transport of EMIMAc out of the fiber during coagulation, which also transports a significant part of the pyrene out of the coagulating fiber. By instead encapsulating

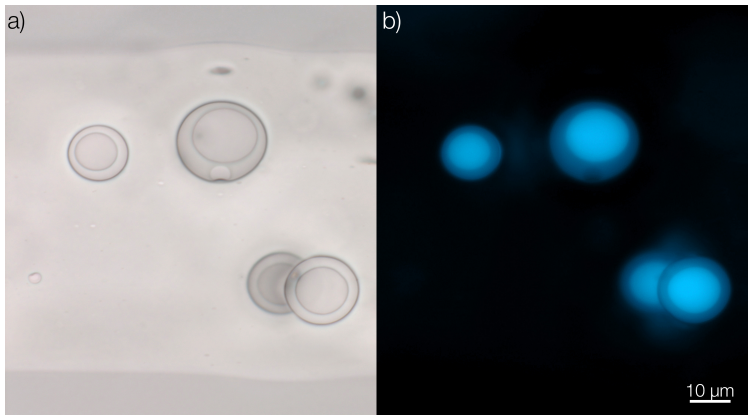

Figure 4.2: A small segment of a wet spun continuous cellulose fiber containing core-shell microcapsules visualized by a) optical and b) fluorescence microscopy. The scale bar is valid for both sub-figures.

pyrene into microspheres, it was protected and this loss of active substance was almost entirely eliminated.

4.1.2 Pyrene release rate from the materials

The release of pyrene from nonwoven fiber materials where the pyrene was surface impregnated, freely dispersed throughout the fiber, and encapsulated into microspheres embedded in the fibers was further evaluated in an aqueous solution. This solution contained the nonionic surfactant Brij L23 in order to establish sink conditions. Apart from the three fiber materials, release measurements were also performed on microspheres not loaded into fiber materials, but directly in a water suspension. The fractional release from these samples is presented in Figure 4.4.

A tremendous difference in the release from the different fiber materials could be seen. Surface impregnation of pyrene resulted in a large burst fraction of approximately 50%. This was likely due to readily available pyrene on the fiber surface that dissolved rapidly. Following this, a slower continuous release was seen until a complete release was achieved after approximately one hour. The second

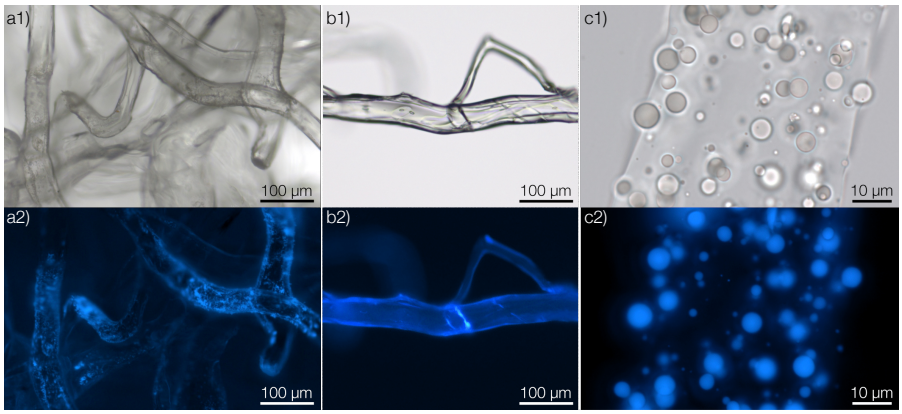

Figure 4.3: Pyrene loaded into nonwoven cellulose fibers by a) surface impregnation, b) freely dispersing throughout fibers and c) microencapsulation in microspheres. Micrographs in a1), b1) and c1) were taken with brightfield illumination, whereas a2), b2) and c2) were taken by fluorescence microscopy.

part in the release was likely the release of pyrene that had entered into the outermost parts of the cellulose fiber during impregnation. This release behavior was modeled mathematically by Equation 3.16 and 3.17. By fitting these equations, an average thickness of 7 µm for the pyrene-containing part of the fiber was found, which was approximately half of the average fiber radius.

For freely dispersed pyrene, the burst release was negligible, and most of the pyrene was released slowly following a diffusion-like release profile over approximately 10 hours. Initially, pyrene should have been homogeneously distributed throughout the fiber, as verified by microscopy in Figure 4.3b2). This release was therefore modeled by a cylindrical geometry as described by Equation 3.12. A diffusion coefficient for pyrene in the cellulose fiber could be fitted from this model. This diffusion coefficient was used when estimating the impregnation depth of the surface impregnated fibers above.

For the microsphere-functionalized fibers, the burst release was negligible as well. Two different approaches to modeling the release was used here. The release was either modeled as a release from microspheres, neglecting the fact that they were immobilized within a fiber. Alternatively, the release was modeled by the cylindrical

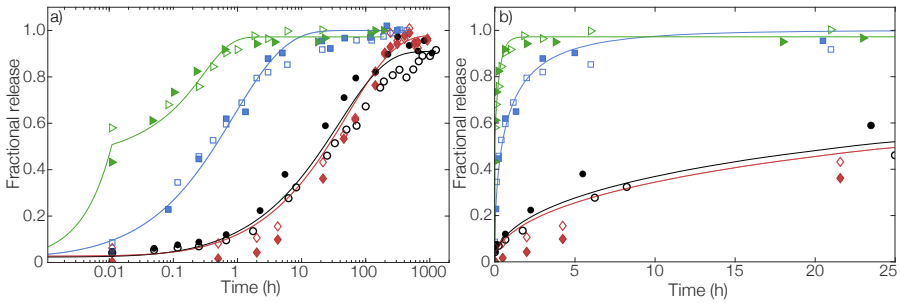

Figure 4.4: Fractional release from fibers containing pyrene loaded by surface impregnation (▷▶), as freely dispersed (□■) and as microencapsulated (◇◆) along with microspheres in water suspension (○●). Solid lines are fits to the appropriate release models. In a) the release is shown on a logarithmic time scale, and in b) the first 25 hours are shown on a linear scale.

geometry of the fibers. In the latter case, the fitted diffusion coefficient would not be the true diffusion coefficient for the material. Rather, it would be an apparent diffusion coefficient given that it was a composite material where the diffusivity of pyrene would differ in the cellulose and PLGA phases respectively.

The fitted (apparent) diffusion coefficients for the different materials are shown in Table 4.1 along with what geometry was used for each model. Comparing the three different materials, an approximately 100-fold decrease in apparent diffusivity was found for the encapsulated pyrene, as compared to freely dispersed. The release rates from microspheres in water and fibers, respectively, were highly similar, meaning that the microspheres acted as the main rate-limiting barrier for the release and not the cellulose matrix.

Table 4.1: Geometries used in fitting diffusion models to the investigated samples, along with fitted apparent diffusion coefficients.

Sample	Geometry	D (m^2/s)
Freely dispersed	Cylinder	$2.02 \cdot 10^{-14}$
Spheres (fiber)	Cylinder	$4.29 \cdot 10^{-16}$
	Sphere	$2.68 \cdot 10^{-18}$
Spheres (susp.)	Sphere	$5.38 \cdot 10^{-18}$

4.2 Triggered Release Systems

Only sustained release from a system may not be sufficient to produce the desired release profile, as described previously. In Paper III, polyphthalaldehyde microcapsules were therefore formulated. The available parameters when formulating the microcapsules were optimized, and the microcapsules were then evaluated as a model system for achieving UV light triggered release.

4.2.1 Formulation

Several parameters can be optimized when formulating microcapsules, such as choice of dispersant and solvent evaporation rate. The choice of dispersant will affect the thermodynamically predicted morphology, as described by the spreading coefficients in Equations 2.2 - 2.5, whereas the solvent evaporation rate instead will affect the kinetics during internal phase separation.

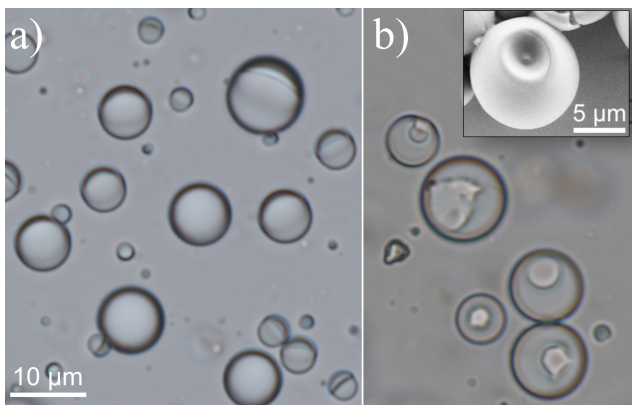

Figure 4.5: Optical micrographs of the microcapsule morphologies obtained when stabilizing with a) PVA and b) PMAA. The inset shows a SEM micrograph of a dried PMAA blueberry microcapsule. The scale bar is valid for both sub-figures.

Two polymeric dispersants were investigated: poly(vinyl alcohol) (PVA) and poly(methacrylic acid) (PMAA). The obtained microcapsule morphologies with these two dispersants are shown in Figure 4.5. Both core-shell and acorn microparticles could be observed in the PVA-stabilized system, whereas a blueberry morphology was obtained when stabilizing with PMAA. To further understand

these morphologies, the spreading coefficients for each system were calculated, Table 4.2. For both dispersants, a value of S_p close to zero was seen. This indicates that both of the systems were on the boundary between a core-shell and an acorn morphology. The high interfacial tension between PPA and pure water further indicates that the polymer is highly hydrophobic. It was the ability of the dispersant to efficiently decrease this polymer-water interfacial tension that drove the formation of core-shell particles and not acorn microparticles. This is uncommon, as it is usually the dispersant's ability to maintain a large oil-water interfacial tension that promotes core-shell formation.

Table 4.2: Interfacial tensions and calculated spreading coefficients for the different dispersants, along with predicted and observed microcapsule morphologies. All values are in mN/m.

Disp.	γ_{ow}	γ_{op}	γ_{pw}	S_p	S_w	S_o	Morphology	
							Predicted	Observed
None	53.5	14.4	43.3	-4.2	-82.3	-24.7	Acorn	-
PVA	21.2	14.4	4.2	2.6	-11.0	-31.5	Core-shell	Acorn Core-shell
PMAA	33.4	14.4	19.4	-0.4	-38.4	-28.5	Acorn	Blueberry

4.2.2 UV Light Exposure

The triggered release from PPA-microcapsules was investigated in two ways: with microcapsules in a water suspension, and microcapsules dried onto a glass substrate. The triggered release from PMAA-stabilized microcapsules in suspension is shown in Figure 4.6. After one minute of UV light exposure, the oil core was seen to start protruding from the cavity in the blueberry microcapsules. After five minutes, the entire oil phase had emerged from the microcapsules. In all capsules, the oil was protruding from the blueberry cavity. It was therefore hypothesized that this was the weakest part of the microcapsule. In terms of triggered release, this designed weakness was highly beneficial since it allowed for a fast and almost instantaneous release of the core contents. Without a blueberry cavity, as was the case for PVA-stabilized microcapsules, no protruding core oil was seen even with longer exposure times. There was, however, a visible deformation of the shell but not to the point where the capsule wall collapsed to release the core oil.

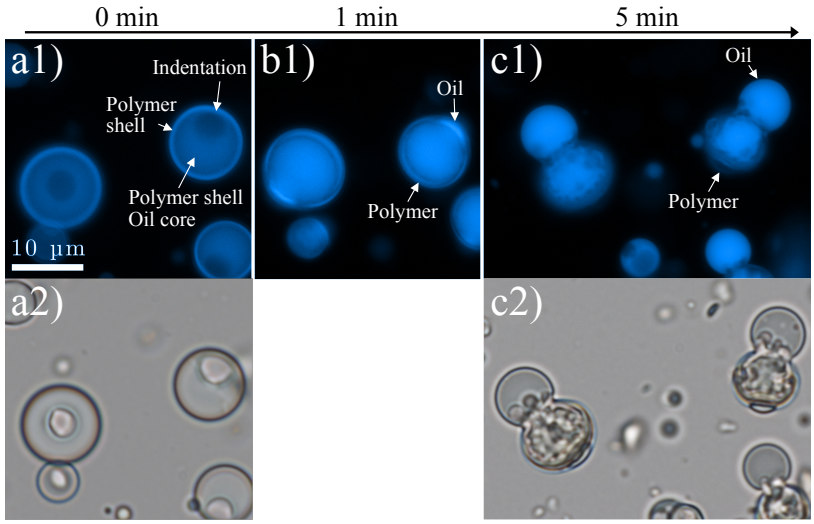

Figure 4.6: *In situ*-triggered release from PMAA-stabilized microcapsules in water suspension after a) 0 min., b) 1 min., c) 5 min. as shown by both fluorescence and brightfield micrographs. The scale bar is valid for all sub-figures.

Apart from microcapsules in water suspension, the triggered release was also evaluated for microcapsules dried onto a glass substrate. PVA-stabilized microcapsules before and after UV light exposure are shown in Figure 4.7. PPA is represented in magenta in the composite micrographs, and the hexadecane oil core is seen in blue. Before exposure, small amounts of oil could already be seen to be not encapsulated. This was most likely due to the fraction of acorn microparticles that were present in the samples. The fraction of the sample that displayed a core-shell morphology was seen as intact particles on the glass. The capsules could be seen to collapse after less than one minute of UV light exposure, causing the core oil to leak out. Despite not showing any triggered release in water suspension, it was clearly possible to trigger a collapse of these microcapsule shells when the particles were in a dry state.

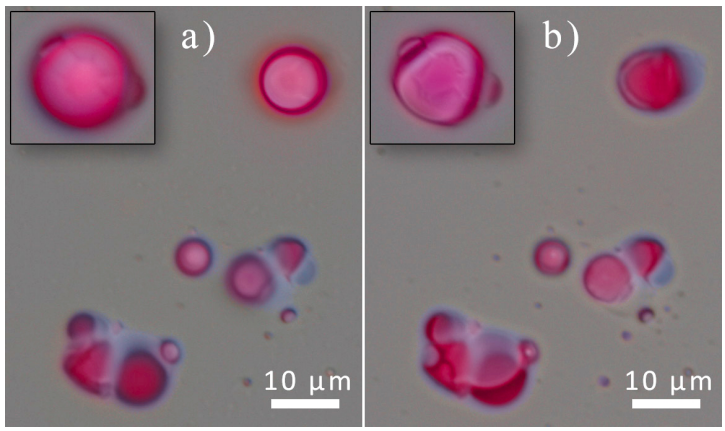

Figure 4.7: PVA-stabilized microcapsules dried onto a glass slide a) before and b) after less than one minute of UV light exposure. In the insets, a magnification of one microcapsule is shown.

5

Concluding Remarks and Future Work

In this thesis, the concept of controlled release has been explored in two different ways for the release of a model hydrophobic substance. Both a slow and sustained release and an instantaneous triggered release were investigated from microparticles. Sustained release microparticles were also incorporated into cellulose fibers, producing a nonwoven material from which a controlled release of the active substance was achieved. After one week, approximately 80% was released, which would be an appropriate release rate in a wound dressing. On the contrary, a significant fractional release could be achieved from the triggered release microcapsules within only minutes after the trigger event. As stated previously, only one controlled release approach may not be sufficient for achieving the desired release profile. Therefore, combinations of sustained and triggered release systems could be imagined for tailoring release profiles.

The release of the hydrophobic model substance pyrene was only investigated in this thesis. This gave a good understanding of material properties and how the release rate can be affected. A proof-of-concept system encapsulating real antimicrobial substances such as isothiazolinones or quaternary ammonium compounds is, however, also desired. The release methodology presented in this thesis could thus be combined with *in vivo*-studies of the antimicrobial efficacy.

The choice of materials could also be further explored. For instance, in a wound care application, both PLGA microparticles and cellulose fibers would be excellent choices of materials for sustained release due to their biocompatibility. This would not be the case for PPA in the case of triggered release. As with the use of pyrene, it was an excellent model system for showing the concept of UV-triggered release, although biocompatible and approved alternatives would be required in a medical application. One interesting class of polymers that fulfills these requirements and shows a pH-triggered degradation and release is polyanhydrides.

Acknowledgments

I would like to thank the Swedish research council Formas for financial support.

There are also several people that I would like to thank for their contributions. My supervisor Lars Evenäs for all of your time and excellent guidance in this project. My co-supervisor Markus Andersson Trojer for your never-ending source of ideas and solutions to my problems. I would also like to thank my examiner Martin Andersson.

Thanks to all my coauthors, Jules Mistral, Ting Yang Nilsson, Hanna Ulmefors, Szilvia Vavra, Gustav Eriksson and Mats Hulander. I hope that we will have more collaborations in the future.

All colleagues at the division of Applied Chemistry are thanked not only for all help, but also for creating a nice working environment.

Finally, I would like to thank friends and family. A special thanks to Elin for all your love and support.

References

[1] T Bjarnsholt et al. “Management of wound biofilm Made Easy”. In: *Wounds International* 8.2 (2017).

[2] Isla Fitridge et al. “The impact and control of biofouling in marine aquaculture: a review”. In: *Biofouling* 28.7 (2012), pp. 649–669.

[3] Diego Meseguer Yebra, Søren Kiil, and Kim Dam-Johansen. “Antifouling technology—past, present and future steps towards efficient and environmentally friendly antifouling coatings”. In: *Progress in organic coatings* 50.2 (2004), pp. 75–104.

[4] AD Russell. “Introduction of biocides into clinical practice and the impact on antibiotic-resistant bacteria.” In: *Journal of Applied Microbiology* 92 (2002), 121S–35S.

[5] James W Readman. “Development, occurrence and regulationof antifouling paint biocides: historical review and future trends”. In: *Antifouling paint biocides*. Springer, 2006, pp. 1–15.

[6] Christopher J Ioannou, Geoff W Hanlon, and Stephen P Denyer. “Action of disinfectant quaternary ammonium compounds against Staphylococcus aureus”. In: *Antimicrobial agents and chemotherapy* 51.1 (2007), pp. 296–306.

[7] Vânia Silva et al. “Isothiazolinone biocides: chemistry, biological, and toxicity profiles”. In: *Molecules* 25.4 (2020), p. 991.

[8] Megan C Jennings, Kevin PC Minbiole, and William M Wuest. “Quaternary ammonium compounds: an antimicrobial mainstay and platform for innovation to address bacterial resistance”. In: *ACS infectious diseases* 1.7 (2015), pp. 288–303.

[9] Munmaya K. Mishra. “Microencapsulation”. In: *Kirk-Othmer Encyclopedia of Chemical Technology*. Wiley, 2019, pp. 1–35. ISBN: 9780471238966.

[10] Rama Dubey. “Microencapsulation technology and applications”. In: *Defence Science Journal* 59.1 (2009), p. 82.

[11] Allan S Hoffman. “The origins and evolution of “controlled” drug delivery systems”. In: *Journal of controlled release* 132.3 (2008), pp. 153–163.

[12] Aaron P Esser-Kahn et al. “Triggered release from polymer capsules”. In: *Macromolecules* 44.14 (2011), pp. 5539–5553.

[13] Markus Andersson Trojer et al. “Encapsulation of actives for sustained release”. In: *Physical Chemistry Chemical Physics* 15.41 (2013), pp. 17727–17741.

[14] Brian Vincent. “Microgels and core-shell particles”. In: *Surface Chemistry in Biomedical and Environmental Science*. Springer, 2006, pp. 11–22.

[15] Andrew Loxley and Brian Vincent. “Preparation of poly (methylmethacrylate) microcapsules with liquid cores”. In: *Journal of colloid and interface science* 208.1 (1998), pp. 49–62.

[16] S Torza and SG Mason. “Three-phase interactions in shear and electrical fields”. In: *Journal of colloid and interface science* 33.1 (1970), pp. 67–83.

[17] Donald C Sundberg et al. “Morphology development of polymeric microparticles in aqueous dispersions. I. Thermodynamic considerations”. In: *Journal of Applied Polymer Science* 41.7-8 (1990), pp. 1425–1442.

[18] Sujit S. Datta et al. “Delayed Buckling and Guided Folding of Inhomogeneous Capsules”. In: *Phys. Rev. Lett.* 109 (13 2012), p. 134302.

[19] Nam Gi Min et al. “Anisotropic microparticles created by phase separation of polymer blends confined in monodisperse emulsion drops”. In: *Langmuir* 31.3 (2015), pp. 937–943.

[20] Tatiya Trongsatitkul and Bridgette M Budhlall. “Multicore–shell PNIPAm-co-PEGMa microcapsules for cell encapsulation”. In: *Langmuir* 27.22 (2011), pp. 13468–13480.

[21] Kathleen J Pekarek, Jules S Jacob, and Edith Mathiowitz. “Double-walled polymer microspheres for controlled drug release”. In: *Nature* 367.6460 (1994), pp. 258–260.

[22] Christian Wischke and Steven P Schwendeman. “Principles of encapsulating hydrophobic drugs in PLA/PLGA microparticles”. In: *International Journal of pharmaceutics* 364.2 (2008), pp. 298–327.

[23] Markus Andersson Trojer et al. “Use of microcapsules as controlled release devices for coatings”. In: *Advances in colloid and interface science* 222 (2015), pp. 18–43.

[24] Susanne Fredenberg et al. “The mechanisms of drug release in poly (lactic-co-glycolic acid)-based drug delivery systems—a review”. In: *International journal of pharmaceutics* 415.1-2 (2011), pp. 34–52.

[25] Chandrashekar Raman et al. “Modeling small-molecule release from PLG microspheres: effects of polymer degradation and nonuniform drug distribution”. In: *Journal of Controlled Release* 103.1 (2005), pp. 149–158.

[26] Alireza Abbaspourrad, Sujit S Datta, and David A Weitz. “Controlling release from pH-responsive microcapsules”. In: *Langmuir* 29.41 (2013), pp. 12697–12702.

[27] Li Liu et al. “Monodisperse core-shell chitosan microcapsules for pH-responsive burst release of hydrophobic drugs”. In: *Soft Matter* 7.10 (2011), pp. 4821–4827.

[28] Kunlin Chen and Shuxue Zhou. “Fabrication of ultraviolet-responsive microcapsules via Pickering emulsion polymerization using modified nano-silica/nano-titania as Pickering agents”. In: *RSC advances* 5.18 (2015), pp. 13850–13856.

[29] Susana Carregal-Romero et al. “NIR-light triggered delivery of macromolecules into the cytosol”. In: *Journal of controlled release* 159.1 (2012), pp. 120–127.

[30] PR Hari, Thomas Chandy, and Chandra P Sharma. “Chitosan/calcium alginate microcapsules for intestinal delivery of nitrofurantoin”. In: *Journal of microencapsulation* 13.3 (1996), pp. 319–329.

[31] Chuji Aso and Sanae Tagami. “Cyclopolymerization of o-phthalaldehyde”. In: *Journal of Polymer Science Part B: Polymer Letters* 5.3 (1967), pp. 217–220.

[32] Hiroshi Ito and C Grant Willson. “Chemical amplification in the design of dry developing resist materials”. In: *Polymer Engineering & Science* 23.18 (1983), pp. 1012–1018.

[33] Feng Wang and Charles E Diesendruck. “Polyphthalaldehyde: Synthesis, derivatives, and applications”. In: *Macromolecular rapid communications* 39.2 (2018), p. 1700519.

[34] Shijia Tang et al. “Low-ceiling-temperature polymer microcapsules with hydrophobic payloads via rapid emulsion-solvent evaporation”. In: *ACS applied materials & interfaces* 9.23 (2017), pp. 20115–20123.

[35] Anthony M DiLauro et al. “Stimuli-responsive core–shell microcapsules with tunable rates of release by using a depolymerizable poly (phthalaldehyde) membrane”. In: *Macromolecules* 46.9 (2013), pp. 3309–3313.

[36] Hiroshi Ito. “Development of new advanced resist materials for microlithography”. In: *Journal of Photopolymer Science and Technology* 21.4 (2008), pp. 475–491.

[37] Byung Soo Kim et al. “BSA-FITC-loaded microcapsules for in vivo delivery”. In: *Biomaterials* 30.5 (2009), pp. 902–909.

[38] Shaoping Sun et al. “pH-sensitive poly (lactide-co-glycolide) nanoparticle composite microcapsules for oral delivery of insulin”. In: *International journal of nanomedicine* 10 (2015), p. 3489.

[39] M Tuncay et al. “Diclofenac sodium incorporated PLGA (50: 50) microspheres: formulation considerations and in vitro/in vivo evaluation”. In: *International journal of pharmaceutics* 195.1-2 (2000), pp. 179–188.

[40] Emma Luong-Van et al. “Controlled release of heparin from poly (ε-caprolactone) electrospun fibers”. In: *Biomaterials* 27.9 (2006), pp. 2042–2050.

[41] Jing Zeng et al. “Influence of the drug compatibility with polymer solution on the release kinetics of electrospun fiber formulation”. In: *Journal of controlled release* 105.1-2 (2005), pp. 43–51.

[42] Narayan Bhattarai, Jonathan Gunn, and Miqin Zhang. “Chitosan-based hydrogels for controlled, localized drug delivery”. In: *Advanced drug delivery reviews* 62.1 (2010), pp. 83–99.

[43] Joshua S Boateng et al. “Wound healing dressings and drug delivery systems: a review”. In: *Journal of pharmaceutical sciences* 97.8 (2008), pp. 2892–2923.

[44] Dieter Klemm et al. “Cellulose: fascinating biopolymer and sustainable raw material”. In: *Angewandte chemie international edition* 44.22 (2005), pp. 3358–3393.

[45] Marguerite Rinaudo. “Chitin and chitosan: Properties and applications”. In: *Progress in polymer science* 31.7 (2006), pp. 603–632.

[46] Marguerite Rinaudo. “Main properties and current applications of some polysaccharides as biomaterials”. In: *Polymer International* 57.3 (2008), pp. 397–430.

[47] CJ Van Oss, RJ Good, and MK Chaudhury. “Additive and nonadditive surface tension components and the interpretation of contact angles”. In: *Langmuir* 4.4 (1988), pp. 884–891.

[48] Kerstin Jedvert et al. “Cellulosic nonwovens produced via efficient solution blowing technique”. In: *Journal of Applied Polymer Science* 137.5 (2020), p. 48339.

[49] Paolo Blasi et al. “Plasticizing effect of water on poly (lactide-co-glycolide)”. In: *Journal of Controlled Release* 108.1 (2005), pp. 1–9.

[50] Carina Olsson et al. “Effect of methylimidazole on cellulose/ionic liquid solutions and regenerated material therefrom”. In: *Journal of Materials Science* 49.9 (2014), pp. 3423–3433.

[51] M. Gibaldi and S. Feldman. “Establishment of sink conditions in dissolution rate determinations. Theoretical considerations and application to nondisintegrating dosage forms”. In: *Journal of pharmaceutical sciences* 56.10 (1967), pp. 1238–1242.

[52] John Crank. *The mathematics of diffusion*. Oxford university press, 1979.

[53] K.J Packer and C Rees. “Pulsed NMR studies of restricted diffusion. I. Droplet size distributions in emulsions”. In: *Journal of Colloid and Interface Science* 40.2 (1972), pp. 206–218. ISSN: 0021-9797.

[54] Michele M Miller et al. “Relationships between octanol-water partition coefficient and aqueous solubility”. In: *Environmental science & technology* 19.6 (1985), pp. 522–529.